Analysis of SST Anomalies in the North Pacific and their Relation to 500 mb Height Anomalies Over the Northern Hemisphere During 1969–1979

By Naoto Iwasaka, Kimio Hanawa and Yoshiaki Toba

Dept. of Geophysics, Tohoku University, Sendai 980 Japan
(Manuscript received 11 June 1986, in revised form 19 November 1986)

Abstract

Characteristics of the SST anomaly field in the North Pacific and their relationship with the 500 mb geopotential height fluctuation in the Northern Hemisphere, were investigated, by using the 5° × 5° grid SST data set for the North Pacific. This data set was newly calculated from the SST data file provided by the Japan Oceanographic Data Center. The typical zonal and meridional scales of the SST anomaly pattern are several and one to two thousands km, respectively. Typical SST anomaly patterns can be traced for several months to a year. Fluctuations with periods of several years are also found in spectral analyses for the SST anomaly field. The SST anomaly tends to appear almost simultaneously over a large area. Clear regularity is not found in the speed and the direction of the migration and/or the expansion of the SST anomaly pattern. However, for restricted periods, the SST anomaly pattern seems to move by advection.

In an EOF analysis of the SST anomaly, the first EOF shows an elliptic monopole spatial pattern centered on the central North Pacific. The time series of the coefficient of the first EOF shows a variation with periods of several months and of two to three years, but has no peak corresponding to the 1972/73 El Niño event. Our results of the EOF analysis are similar to those of Davis (1976), but somewhat different from Weare *et al.* (1976) and Kawamura (1984) because of differences in the domain of the analyses.

The SST fluctuations are highly correlated with 500 mb height variations in the Northern Hemisphere. We could conclude based on the lag correlation analysis that the SST anomalies represented by the first EOF are caused by the 500 mb height fluctuation corresponding to the PNA pattern.

1. Introduction

The sea surface temperature (SST) reflects the upper ocean thermal condition and its fluctuations are related not only to the variations in the oceanic upper layer but also to atmospheric fluctuations. Therefore, it is important to investigate the SST anomaly variation in order to improve the understanding of the global scale ocean-atmosphere interactions.

In the previous studies, the characteristics of the large scale SST anomaly fluctuations have been investigated by, for example, Favorite and McLain (1973), Iida *et al.* (1974), Iida *et al.* (1975), and Nishihashi and Imai (1985) by using the SST anomaly maps and through correlation analyses and by, for instance, Barnett and Davis (1975), Davis (1976), Weare *et al.* (1976), Hsiung and Newell (1983), and Kawamura (1984) through the empirical orthogonal function (EOF) analyses. Michaelsen (1982) studied the phase propagation of SST anomaly through the frequency domain principal component analysis (FDPC). On the other hand, statistical analyses of the SST anomaly variation were studied by, for example, Namias and Born (1970) and Namias (1970), in which they performed the autocorrelation analysis.

White and Walker (1974), White *et al.* (1980), Barnett (1981), White *et al.* (1982), and White *et al.* (1985), for example, studied on the re-

lationship between the SST and the oceanic subsurface conditions through the data obtained from the ocean weather stations, XBT and AXBT data, BT observations and hydrographic data. The SST variation related to the fluctuation of the oceanic fronts was also studied, for example, by Saur (1980). Studies on the development of the ocean mixed layer which closely related to the SST variation were carried out by Elsberry and Camp (1978), Elsberry and Garwood (1978) and Elsberry and Raney (1978).

The empirical relationships (partly including the physical process, *e.g.*, the Ekman drift current) between the SST fluctuation and the atmospheric variation have been researched by, for example, Roden and Groves (1960), Namias (1959, 1971, 1973, 1975), and Davis (1976), in which they have attempted to simulate the SST anomaly based on the atmospheric conditions.

In the view of the relationships between the global scale atmospheric fluctuations and the large scale SST anomaly variation, Namias (1969, 1971, 1978, 1980), Dickson and Namias (1976), and Douglas *et al.* (1982), for example, investigated the SST fluctuation in the middle latitude. Lanzante (1984) and Love (1985) studied the relation between the SST and the atmospheric condition with the method proposed by Prohaska (1976). In Kawamura (1984, 1986), correlation analyses between the EOFs and sea level pressure (SLP), 500 mb geopotential height were carried out. There are also a lot of numerical studies of the SST, *e.g.*, Reynolds (1978), Frankignoul and Reynolds (1983), and Pitcher *et al.* (1986). Recently, Frankignoul (1985) reviewed the studies of the SST anomaly and large scale atmospheric fluctuation, and also air-sea feed back in the middle latitude.

The purposes of the present study are to describe the characteristics of the dominant SST anomaly pattern in the North Pacific by using the newly developed SST data set, and to find the relation between the dominant SST anomaly fluctuation in the North Pacific and the atmospheric nonseasonal variation over the Northern Hemisphere with the view point that the large scale SST fluctuations are the manifestation of the variations of the global scale ocean-atmosphere system.

The presentations of the study are as follows. The data and data processing procedures will be described in Section 2. In Section 3, characteristics of the SST anomaly in the North Pacific will be shown. In Section 4 EOF analysis of the SST anomaly and in Section 5 relationships between the 500 mb height fluctuation in the Northern Hemisphere and the dominant SST anomaly pattern in the North Pacific will be shown.

2. Data and data processing

SST data

The original data provided by the Japan Oceanographic Data Center (JODC) cover the Pacific Ocean between 60°N and 30°S for the period from 1945 to 1981. These data include those by both the intake observations and the bucket observations. Though the difference between these two observation methods has been pointed out in previous studies (*e.g.*, Barnett, 1984), we ignored the difference because this effect is not thought to be serious for the purpose of the present study. We used the data in the North Pacific during the period from 1969 to 1979, since there were very few data during 1945–1968 and after 1979, and in the southern hemisphere.

Before making the data sets, we eliminated apparently erroneous data which had values above 35.0°C or under –2.5°C. After the long-term monthly mean SST and the monthly standard deviation (sigma) for each Marsden Square (MSQ) were calculated, the data of SST were also removed whose deviations from the long-term monthly mean values were beyond three times sigma.

5° x 5° SST data set

We calculated the monthly mean SST averaged for 5° (latitude) x 5° (longitude) grid for the North Pacific during the period from 1969 to 1979. This averaging scale in space was employed in order to avoid the contamination by mesoscale fluctuations, which especially dominate in the western North Pacific (White and Bernstein, 1979). The procedures used to calculate the 5° x 5° data set are as follows: First, the SST data were averaged for 1° (latitude) x 5° (longitude) grid for each month in order to reduce the distortion of the 5° x 5° averaged values caused by inhomogeneous spatial distri-

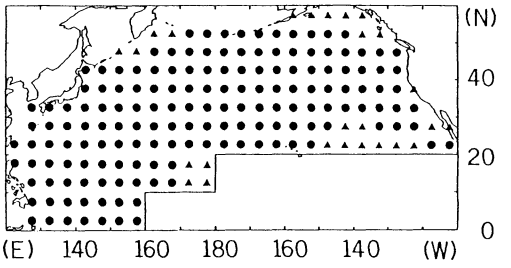

Fig. 1. Array of the 5° x 5° SST data set. Black circles indicate the grid points which have 132 continuous months (1969–1979) values, and triangles are the grid points which have some lacks of data.

bution of the data. In the case in which a 1° x 5° grid had no value, and when there were at least two adjacent grids with their values or when both the preceding and the following months of the same grid had their values, the value was filled by an interpolation from these values. Then, the 5° x 5° grids were represented by the averages of the five 1° x 5° grid values included in each 5° x 5° box. In the case in which a 5° x 5° grid had still no value, a similar interpolation was made as the case of 1° x 5° grid.

The array of the 5° x 5° grid points finally used for the analyses is shown in Fig. 1.

500 mb geopotential height data

Monthly mean 500 mb geopotential height data for the Northern Hemisphere for the period from 1968 to 1980 were provided by Mr. H. Nakamura (Tohoku Univ., now at Univ. of Washington). Monthly mean values were calculated by him for the NMC (National Meteorological Center) grid from daily 1200 GMT 500 mb geopotential height data from theNational Center for Atmospheric Research (NCAR) library.

3. Characteristics of the SST anomaly field in the North Pacific

We define the SST anomaly as the residual obtained after subtracting the 11-year (1969–1979) monthly mean value from the monthly mean SST value for each month.

SST anomaly maps and time-longitude and time-latitude diagrams of the SST anomaly

In order to describe the spatial and temporal characteristics of the SST anomaly pattern in the North Pacific, the 132 monthly SST anomaly maps over the North Pacific from January 1969 to December 1979, the time-longitude and time-latitude diagrams were drawn. The latter diagrams show the temporal fluctuations of the SST anomaly along a particular latitude plotted on the time versus longitude graph, and along a given meridian, respectively. In Fig. 2, the time-longitude diagrams for 32.5°N and 42.5°N are shown (the time-latitude diagrams are not shown here).

The general characteristics of the temporal variation of the SST anomaly are described as follows from the observation of its distribution on the monthly SST anomaly maps and the time-longitude and the time-latitude diagrams: (1) The SST anomaly appears over a large span almost simultaneously, and a quarter or a half of the area of the North Pacific is covered by one anomaly pattern with the same sign. (2) The amplitude of the SST anomaly is large (~ 2.0°C) in the region north of 40°N, off Hokkaido, Japan, and in the region east of 160°W. (3) An anomaly pattern can usually be traced for several months to a year. Long-term fluctuations are shown with periods of several years in the time-longitude and time-latitude diagrams. (4) The zonal scale of the anomaly pattern is several thousands km, and the meridional scale is one to two thousands km. (5) Clear regularity is not found in the speed and the direction of the migration and/or the expansion of the SST anomaly pattern in this period. However, the migration and/or the expansion tend to be directed zonally in usual cases.

Nishihashi and Imai (1985) showed the seasonally averaged SST anomaly maps for the Pacific Ocean for 1972, from 1976 to 1978 and from 1982 to 1983. In their figures also clear regularity was not found in the migration and/or expansion of the SST anomaly pattern. On the other hand, Favorite and McLain (1973) showed that the SST anomaly patterns moved anticyclonically along the North Pacific subarctic gyre with the period of 5–6 years. Namias (1970) insisted through the correlation analysis that the SST anomaly moved along the subtropical gyre. However, movement of the SST anomaly pattern is rather random in the present study. Michaelsen (1982) showed from the FDPC analysis that the phase of the SST anomaly fluctuation with the frequency of 0.02 cycle per month (cpm) moved

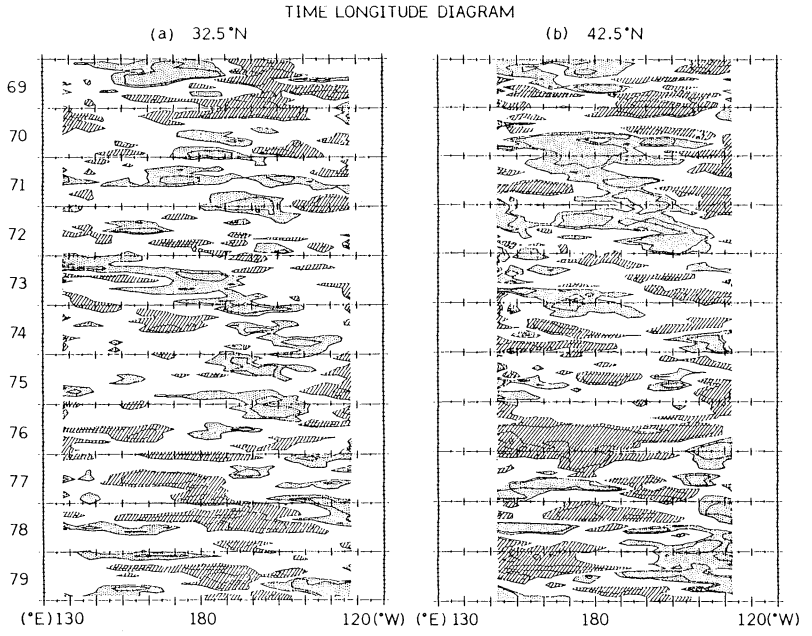

Fig. 2. Time-longitude diagrams of the SST anomaly; (a) 32.5°N and (b) 42.5°N. Hatched area indicates the SST anomaly which is below −0.5°C, and dotted area above +0.5°C. Contour interval is 0.5°C.

eastward along the midlatitude of the North Pacific. However, we could not verify the above result by Michaelsen (1982) because the length of the data set was not enough to analyze for the variation with frequency of 0.02 cpm.

Despite the characteristics mentioned in (5), in Fig. 2, for restricted periods, we can find the migration of the anomaly pattern in the eastwest direction. For example, in the period from the end of 1970 to the end of 1972, the positive anomaly pattern along 42.5°N moved from 170°E to 150°W with repeating the change in amplitude, *i.e.*, strong in autumn and winter, and weak in spring and summer. The migration speed of this pattern was about $6 \cdot 10^{-2} \mathrm{m \cdot s^{-1}}$ (0.1 knot), which seems to be rather smaller than the current speed in this area, but this movement of the anomaly pattern is probably caused by advection of the North Pacific subarctic gyre.

SST anomaly spectra

The SST anomaly spectrum was calculated for each 5° x 5° grid points in order to describe the characteristics of the temporal SST anomaly fluctuations. The Maximum Entropy Method (the number of prediction-error filter term was 20) was used to calculate the spectra because of advantage in treating short-length time series such as the SST anomaly in the present study. The SST anomaly spectra for several grids are shown in Fig. 3.

The general features of the SST anomaly spectrum for each grid point are as follows: (1) There are several peaks in the frequency band from 0.1 to 0.5 cpm and one peak in from 0.01 to 0.1 cpm band. (2) In the frequency band below 0.01 cpm band, the grid points at which the spectral density increases with decreasing frequency, are distributed in the middle and eastern part of the North Pacific and along the Aleutian Islands and off the west coast of the North America (Fig. 3a, b). (3) The grid points with a high peak in from 0.01 to 0.1 cpm band are found in almost all area, especially in the middle and the western part of the North Pacific (Fig. 3b, c). Frequency of this peak is about from 0.028 cpm (period of about 3 years) to 0.056 cpm (1.5 years). (4) Each grid point has several peaks in the frequency band higher than 0.1 cpm, though these peaks are not so significant. (5) In lower latitude, some grid points have near-white spectrum (Fig. 3d).

In the previous studies, Iida *et al.* (1974), in which the SST anomaly in the western North

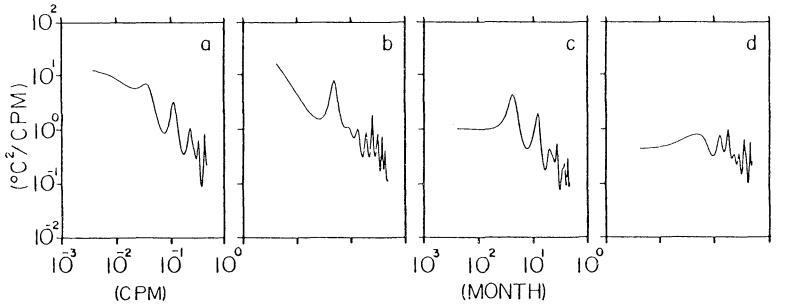

Fig. 3. Spectra of the SST anomaly for the grid points of (a) 42.5°N, 137.5°W, (b) 42.5°N, 177.5°E, (c) 37.5°N, 152.5°E, and (d) 7.5°N, 142.5°E.

Pacific during the period from 1956 to 1970, showed the SST anomaly spectra for 5° x 5° grid points in the region south and east to Japan Islands. They showed that the spectral peaks with the period of 5 to 7.5 years and 1 to 1.5 years were found in almost area, in which they are strong in the northeastern area off Japan and the east coast of Hokkaido. However, the significant peaks with the period of 2 to 3 years were found only in the region off the east and south coast of the Japan Islands. These features are somewhat different from the results in the present study. These differences might be caused by the difference in the period for analysis. Saiki and Nagasaka (1986) studied the regional mean SST anomaly and their spectra for the North and Equatorial Pacific. They found the 6 year-period peak in all region and the 3.5 year-period peak in the equatorial region. In the eastern part of the North Pacific they also found the peak with the period of 10.5 years. The peaks of about from 3 to 1.5 year-period are found in the western region between 10°N to 35°N and in the eastern part. The 6 year-period fluctuations in the SST anomaly are generally found in the North Pacific, but in the present study such frequency variation was unable to be detected as the sharp peak because of the shortness of the time series; frequency band lower than 0.01 cpm in the present study probably include the energy of the fluctuation with the period of 6 years.

4. EOF analysis of the SST anomaly

We applied an EOF analysis to the SST anomaly field in the North Pacific in order to extract the dominant spatial/time variation pattern of the anomaly field. There are several kinds of EOF analysis techniques, *i.e.*, the Covariance Method in which the EOFs are decomposed from the covariance matrix of SST anomalies, and the Cross Correlation Method in which the cross correlation matrix is used. In the present study, we applied the Covariance Method because by using this method, one can extract not only the dominant spatial pattern but also can show the location of specific regions with high variance relative to the rest of the field.

The data set used for the EOF analysis is 5° (latitude) x 10° (longitude) mean monthly SST anomaly data set, because if we used the 5° x 5° data set with the number of grid points much larger than the number of samples, the rank of covariance matrix would be reduced so that the low-indexed sample eigenvalue might be overestimated and the high-indexed underestimated (Storch and Hannoschöck, 1985). Each grid point value was calculated by averaging the two grids of the 5° x 5° SST data set in the same latitude in each MSQ box. This averaging procedure was based on the results in Section 3 that the spatial scale in east-west direction is about twice larger than that in north-south direction.

The first nine of the EOFs of the SST anomaly are beyond the 95% confidence interval of the noise EOFs which was estimated with the selection rule N proposed by Preisendorfer *et al.* (1981). However, in the third and fourth EOFs and in from the fifth through the ninth EOFs, effective degeneracies and mixings may occur because the sampling errors in eigenvalues of these EOFs are larger than the distance to neighbouring eigenvalue (North *et al.*, 1982). Ultimately, we will discuss only the first and the second EOFs in the present study.

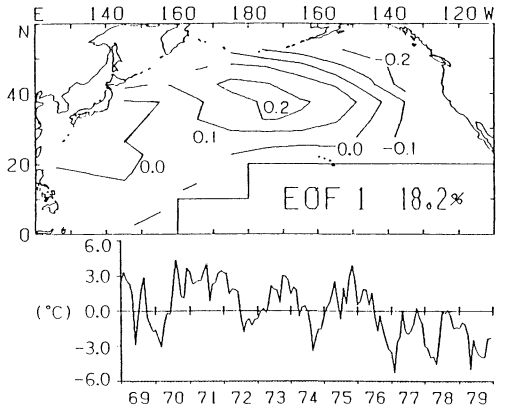

Fig. 4. Spatial pattern and the time series of coefficient of the first EOF of the SST anomaly in the North Pacific.

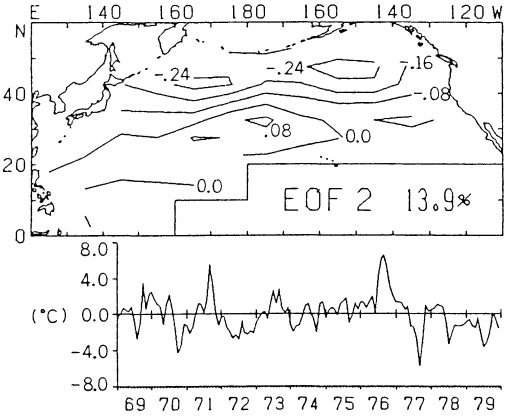

Fig. 5. Same as Fig. 4, except for the second EOF.

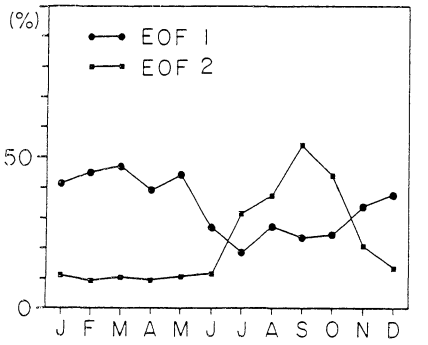

Fig. 6. Seasonal contribution indices (SCI) of the first and the second EOFs. The definition of SCI is referred to the text.

The spatial pattern of the first EOF (18.2% of total variance) is an elliptic monopole pattern with the center at 37.5°N, 177.5°E as shown in Fig. 4. The second EOF (13.9%) has the north-south pattern, having the node along about 35°N line as shown in Fig. 5. The time series of coefficients of the first two EOFs show the variations with periods of several months and two to three years.

It is noticeable that in the El Niño period from the end of 1972 to the beginning of 1973 there is no contribution of the first EOF, *i.e.*, no remarkable peak in the time series of coefficients. On the other hand, in the time series of the second EOF, remarkable peaks appeared in the summers of 1971, 1976 and 1977.

In order to describe the seasonality of each EOF, the seasonal contribution index (SCI) was defined as follows:

$$Ci(M)=\frac{\sum_{y=1969}^{1979} f_i^2(My)}{\sum_{j=1}\sum_{y=1969}^{1979} f_j^2(My)}$$

where $Ci\,(M)$ is the seasonal contribution index (SCI) of the i-th EOF for the M-th calendar month (January, February, etc.), and $f_i\,(My)$ is the coefficient of the i-th EOF for the value of the M-th month of the year y (1969 to 1979). Seasonal variation of SCI is shown in Fig. 6.

It is clear from Fig. 6, that the first EOF is dominated in from January to May and December whereas the second EOF is prevailing from July through October. That is, it can be said that the first EOF is the winter-season mode and the second EOF the summer-season mode.

Comparing with previous studies for the first EOF, the results of the present study primarily agree with those of Barnett and Davis (1975) and Davis (1976). Spatial pattern of the first EOFs of Weare *et al.* (1976), Hsiung and Newell (1983), and Kawamura (1984) also resemble that of the present study focusing on the area corresponding to the present study. The time series of coefficient of the first EOF in the present study is, however, somewhat different, in the period from 1972 to 1974, from those of Weare *et al.* (1976) and Kawamura (1984), in which their first EOFs were dominated by the signal of *every* El Niño events. Such difference is also found in the period from 1951 to 1954 in comparing with the results of Davis (1976) and those of Weare *et al.* (1976) and Kawamura (1984).

For the second EOF, the spatial pattern of the present study resembles those of Barnett and Davis (1975) and of Davis (1976). The time series of the coefficient is, however, not shown in their studies. The second EOFs of Weare *et al.* (1976) and Kawamura (1984) are quite different from that in the present study.

These differences between Weare *et al.* (1976), Kawamura (1984) and the present study were primarily caused by the area selected as the object of the study, *i.e.*, their study included the central and eastern part of Equatorial Pacific. The method of EOF analysis in Kawamura (1984), *i.e.*, the Cross Correlation Matrix method, also might cause the difference.

The differences among the results of the present study and those of Weare *et al.* (1976) and Kawamura (1984) suggest that the dominant mode of SST anomaly fluctuation in the North Pacific is *not always* coherent with that in the Equatorial Pacific Ocean. That is, negative SST anomaly does *not always* appear in the North Pacific during the El Niño event period. In fact, negative SST anomaly did not appear in the middle North Pacific during the period from the end of 1972 to the beginning of 1973 in the SST anomaly maps of the present study and also in those of Nishihashi and Imai (1985), Emery and Hamilton (1985), for example.

The SST anomalies in the summer of 1971, 1976, and 1978, which represented by the second EOF, are thought to be restricted in thin surface layer because the second EOF is the summer-season mode, and because duration of these anomalies were up to 3 months. Actually, White *et al.* (1980) showed the upper ocean thermal anomaly state during September 1976 to August 1978 for the eastern part of the North Pacific. These anomalies were probably generated by external-forcing anomaly such as heat flux anomaly at the sea surface (including cloudiness and/or insolation anomaly).

5. Relationships between the results of EOF analysis for the SST anomaly and the 500 mb height anomaly fluctuation

In this section, we will discuss the correlation analysis between the 500 mb geopotential height anomaly in the Northern Hemisphere and the time series of coefficient of the EOFs for the SST anomaly in the North Pacific.

Fluctuations of the 500 mb geopotential height field are often used as one of the manifestations of the tropospheric activity. Since the tropospheric variation over the extratropical latitude ocean shows a highly barotropic structure, especially in winter (Blackmon *et al.*, 1979), the SLP variation has a high correlation with the 500 mb height fluctuation. Moreover, previous studies on the atmospheric teleconnection have often been performed by using 500 mb height field data (Wallace and Gutzler, 1981, etc.).

We define the monthly 500 mb geopotential height anomaly as the residual obtained after subtracting the 13-year mean (from 1968 to 1980) monthly value from the monthly mean 500 mb geopotential height value of each NMC grid for each month.

In order to test the significance of the results in correlation analysis, the Monte Carlo simulation was performed. In this simulation we calculated correlation coefficients between the time series of the EOFs and artificially generated time series using the Marcov process formula

$$X_i = A X_{i-1} + n_i$$

where A is the autocorrelation at a lag of one month and n_i is white noise at time $t = i$ (months). Coefficient A is to be determined from the autocorrelation function of monthly 500 mb height anomalies. Then, the rejection region where the hypothesis of $\rho = 0$ (ρ is the correlation coefficient of universe) is to be rejected is estimated based on the distribution of correlation coefficients calculated above. In the present study, A was estimated by calculating sample autocorrelations for several grid points of 500 mb height data and values of 0.3 ~ 0.6 were obtained. The simulation was carried out for $A = 0.3$, $A = 0.4$, $A = 0.5$, and $A = 0.6$, and showed that the rejection regions with 10% significance level were greater than 0.18 for $A = 0.3$, 0.20 for $A = 0.4$, 0.22 for $A = 0.5$, and 0.25 for $A = 0.6$, respectively.

Figure 7 shows the spatial distribution pattern of correlation coefficients (from now on, referred to as correlation pattern) between the time series of coefficient of the first EOF and the 500 mb height anomaly field fluctuation with no time lag. A remarkable feature is a wavelike pattern, in which negative coefficients distributing in sub-

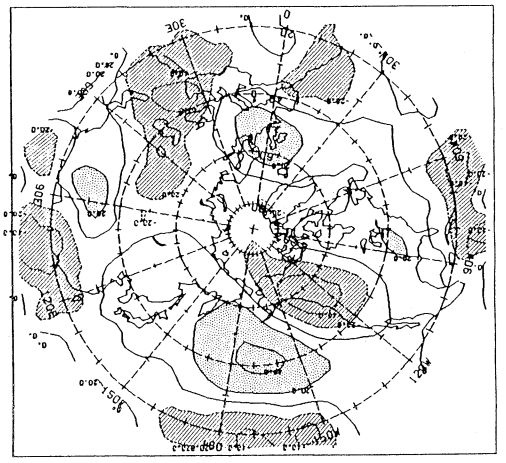

Fig. 7. Correlation pattern between the time series of coefficient of the first EOF and the 500 mb geopotential height anomaly fluctuation in the Northern Hemisphere with no time lag. Hatched area indicates the correlation coefficients which are below −0.2, and dotted area above +0.2. Contour interval is 0.2.

tropical latitude over the Pacific, positive over the central and eastern North Pacific, and again negative over Alaska and the east coast of Canada. This pattern is identified with the Pacific/North American (PNA) teleconnection pattern (Wallace and Gutzler, 1981). It is worthwhile to note that the correlation pattern for the first EOF non-dominant season (June to November, see Fig. 5) reveals also a weak PNA-like pattern (not shown here).

Figure 8 shows the results of lag correlation analysis. The correlation pattern over the North Pacific with lag of −1 month (the atmosphere leads the ocean by one month) also clearly shows the PNA pattern, whereas no significant pattern appears over the North Pacific for the lag of +1 month. This contrast between these figures is striking. The highest correlation is found in lag of −1 month though the PNA pattern is seen in lag of −2 and −3 months.

Relationships between the PNA pattern and the SST anomaly in the North Pacific are also confirmed by the correlation analysis between the SST anomaly and the PNA index defined by Wallace and Gutzler (1981). Correlation patterns resembling the spatial pattern of the first EOF (not shown here) are clearly shown for the first EOF dominant season (January to May and December). The highest correlation coefficients, $\rho = -0.53$ at middle of the North Pacific and $\rho = 0.57$ at near the west coast of the North America, are obtained for lag of −1 month (atmosphere leads to ocean). Weak correlation pattern resembling the first EOF is also shown for the first EOF non-dominant season.

These results shows that the SST anomaly fluctuation represented by the first EOF is caused by the atmospheric variation corresponding to the PNA pattern. Lag association, *i.e.*, atmospheric fluctuation precedes the SST anomaly variation in the North Pacific, has been also supported by both statistical researches (*e.g.*, Davis, 1976; Lanzante, 1984) and numerical experiments (*e.g.*, Pitcher *et al.*, 1986).

The results of the correlation analysis for the

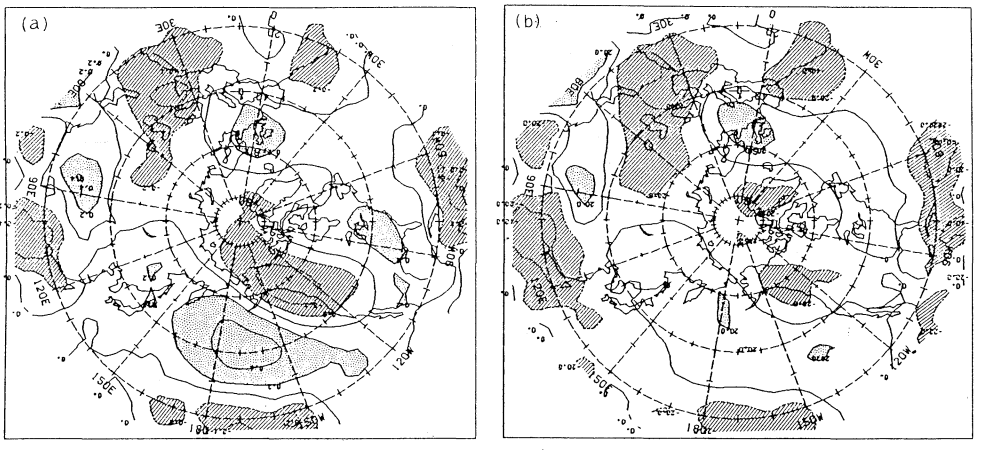

Fig. 8. Lag correlation patterns between the first EOF and the 500 mb height; (a) lag of −1 month (the atmosphere leads the ocean), (b) lag of +1 month.

time series of the second EOF with no time lag (not shown here) shows the correlation pattern which is like the north-south oscillation with a node on about 40°N latitude line. This correlation pattern, however, is rather weak and restricted to the western North Pacific sector.

In the previous studies, Horel and Wallace (1981) and Kawamura (1984) also showed the PNA pattern for the correlation between the values in the Northern Hemisphere winter (or February) of the time series of the first EOF obtained from the Pacific SST anomaly including the equatorial region and the geopotential height anomaly over the Northern Hemisphere. Since the time series of their first EOF primarily represents the SST anomaly in the eastern Equatorial Pacific, their results showed the relationship between the eastern Equatorial Pacific SST and the Northern Hemisphere in winter. Combining their results with that in the present study, it is concluded that in winter the SST anomaly in the North Pacific can be affected by that fluctuation in the equatorial region through the atmospheric variation corresponding to the PNA pattern. It is also shown in Dickson and Namias (1976) and Lanzante (1984) that the PNA pattern is related to the SST anomaly pattern resembling the first EOF in the present study. These results shown in previous studies are the interannual relationship for particular season between the dominant SST anomaly pattern in the North Pacific and the atmospheric fluctuation over the Northern Hemisphere, whereas the results presented here include the relation of both interannual and intermonthly fluctuations. Actually, Blackmon *et al.* (1984) and Esbensen (1984) revealed that the PNA teleconnection pattern has a wide frequency band.

6. Summary and Discussion

In the present study, we have shown the characteristics of the SST anomaly in the North Pacific, and the relationships between the SST anomaly and the 500 mb height anomaly in the Northern Hemisphere. The general characteristics of the SST anomaly in the North Pacific are as follows: zonal and meridional scales are several thousands km, and one to two thousands km, respectively. The anomaly pattern can be traced for several months to a year. The fluctuations with period of several years are also found. The SST anomaly almost simultaneously appears at a large area. Clear regularity is not found in the speed and the direction of the migration and/or the expansion of the SST anomaly pattern. For restricted periods, however, the SST anomaly seems to move by advection.

The dominant SST anomaly pattern in the North Pacific, which is represented by the first EOF, has an elliptic monopole spatial pattern centered in the central North Pacific. The time series of coefficient of this pattern shows the variation with periods of several months and of two to three years, but has no peak corresponding to the 1972/73 El Niño event. This result implies that the SST anomaly in the North Pacific is *not always* connected with the El Niño events during the ENSO periods.

The dominant SST anomaly fluctuation represented by the first EOF is highly correlated with the atmospheric variation identified with the PNA pattern. Lag associations between the first EOF and the PNA pattern suggest that the dominant SST anomaly pattern in the North Pacific is caused by the PNA teleconnection pattern.

Reappearance of the SST anomaly of the same sign in successive years in Fig. 2 suggests that the ocean retains the heat content anomaly in the subsurface water over successive years, because the SST in winter can be strongly affected by the oceanic subsurface state due to deepening of surface mixed layer in winter. Weakening of the SST anomaly in warm season is caused by formation of the thin seasonal surface layer which obstructs the connection of the SST and the subsurface layer. This inference is supported by previous studies: White and Walker (1974) showed thermal variations in the ocean subsurface layer with the period from one to several years existed and the phase propagated from surface to interior using the ocean ship observations, and White *et al.* (1980) showed that anomalous thermal condition in the oceanic subsurface layer retained over successive years.

It is difficult to estimate main processes contributing to development of the large scale SST anomaly because of limits of the data in the present study. Based on the previous studies, however, it is considered that most important pro-

cesses are turbulent vertical mixing forced by wind stress and heat flux at sea surface; most part of both processes are induced by strong atmospheric storm events (Elsberry and Garwood, 1978; Elsberry and Camp, 1978; Elsberry and Raney, 1978). In fact, in the winter of 1976/1977 when large negative SST anomaly appeared in the middle of the North Pacific (see Fig. 11 of Namias, 1978), cyclone activity in the northern part of the North Pacific (or the Aleutian Low activity) was more intense than usual (Namias, 1978; Emergy and Hamilton, 1985) and White *et al.* (1980) showed that strong vertical mixing occurred in the middle of the North Pacific. This inference is also supported by numerical experiments of Frankignoul and Reynolds (1983) and Haney (1985). Although the Ekman current may also contribute to the formation of the SST anomaly, Namias (1959), Roden and Groves (1960) and Clark (1972), for example, did not succeed to explain the SST anomaly or its change with this process quantitatively. The Ekman pumping effect induced by the large scale wind system is negligible (White *et al.* 1980). However, anomaly of large scale wind stress curl may cause the change in the SST field through the fluctuation of the front or rim of wind-driven circulation system.

All results in the present study indicate that the large scale SST anomaly fluctuations is one aspect of the variation in the global scale ocean-atmosphere system.

Acknowledgements

We are grateful to Mr. H. Nakamura (Upper Atmosphere and Space Research Laboratory, Tohoku Univ., now at Univ. of Washington) who kindly provided us the monthly mean 500 mb geopotential height data for the Northern Hemisphere and advised us on the meteorological aspects of the present study. He also gave us some programs used in the present study. In the present study, the SST data for the Pacific Ocean was provided by the Japan Oceanographic Data Center (SST file 84–040–1, 2, 3). This work was supported by a Grant-in-Aid for Co-operative Research, by the Ministry of Education, Science and Culture, project No. 58340027 (Pre-OMLET).

References

Barnett, T.P., 1981: On the nature and cause of large-scale thermal variability in the central North Pacific Ocean. *J. Phys. Oceanogr.*, **11**, 887–904.

———, 1984: Long-term trends in surface temperature over the oceans. *Mon. Wea. Rev.*, **112**, 303–312.

———, and R.E. Davis 1975: Eigenvector analysis and prediction of sea surface temperature fluctuations in the North Pacific Ocean. *Proc. WMO/IAMAP symposium on long-term climatic fluctuations*, 439–450.

Blackmon, M.L., R.A. Madden, J.M. Wallace, and D.S. Gutzler, 1979: Geographical variations in the vertical structure of geopotential height fluctuations. *J. Atmos. Sci.*, **36**, 2450–2466.

———, Y.-H. Lee, and J.M. Wallace, 1984: Horizontal structure of 500 mb height fluctuations with long, intermediate and short time scales. *J. Atmos. Sci.*, **41**, 961–979.

Clark, N.E., 1972: Specification of sea surface temperature anomaly patterns in the eastern North Pacific. *J. Phys. Oceanogr.*, **2**, 391–404.

Davis, R.E., 1976: Predictability of sea surface temperature and sea level pressure anomalies over the North Pacific Ocean. *J. Phys. Oceanogr.*, **6**, 249–266.

Dickson, R.R., and J. Namias, 1976: North American influences on the circulation and climate of the North Atrantic sector. *Mon. Wea. Rev.*, **104**, 1255–1265.

Douglas, A., D. Cayan, and J. Namias, 1982: Large-scales in North Pacific and North American weather patterns in recent decades. *Mon. Wea. Rev.*, **110**, 1851–1862.

Elsberry, R.L., and N.T. Camp, 1978: Oceanic thermal response to strong atmospheric forcing. I. Characteristics of forcing events. *J. Phys. Oceanogr.*, **8**, 206–214.

———, and R.W. Garwood, Jr., 1978: Sea-surface temperature anomaly generation in relation to atmospheric storms. *Bull. American Meteor. Soc.*, **59**, 786–789.

———, and S.D. Raney, 1978: Sea surface temperature response to variations in atmospheric wind forcing. *J. Phys. Oceanogr.*, **8**, 881–887.

Emery, W.J., and K. Hamilton, 1985: Atmospheric forcing of interannual variability in the northeast Pacific Ocean: connections with El Niño. *J. Geophys. Res.*, **90**, 857–868.

Esbensen, S.K., 1984: A comparison of intermonthly and interannual teleconnections in the 700 mb geopotential height field during the Northern Hemisphere winter. *Mon. Wea. Rev.*, **112**, 2016–2032.

Favorite, F., and D.R. McLain, 1973: Coherence in transpacific movements of positive and negative anomalies of sea surface temperature. 1953–60. *Nature*, **244**, 139–143.

Frankignoul, C., 1985: Sea surface temperature anomalies, planetary waves, and air-sea feedback in the middle latitudes. *Rev. Geophys.*, **23**, 357–390.

———, and R. Reynolds, 1983: Testing a dynamical model for midlatitude sea surface temperature anomalies. *J. Phys. Oceanogr.*, **13**, 1131–1145.

Haney, R.L., 1985: Midlatitude sea surface temperature anomalies: a numerical hindcast. *J. Phys. Oceanogr.*, **15**, 787–799.

Horel, J.D., and J.M. Wallace, 1981: Planetary-scale atmospheric phenomena associated with the Southern Oscillation. *Mon. Wea. Rev.*, **109**, 813–829.

Hsiung, J., and R.E. Newell, 1983: The principal nonseasonal modes of variation of global sea surface temperature. *J. Phys. Oceanogr.*, **13**, 1957–1967.

Iida, H., K. Katagiri, and I. Maeda 1974: On the changes of sea surface temperature in the western North Pacific Ocean. *Oceanogr. Mag.*, **25**, 73–88.

———, K. Katagiri, I. Maeda, and E. Kamihira 1975: On the normals of monthly sea surface temperatures from 1956 to 1970 for 5-degree squares in the western North Pacific Ocean. *Oceanogr. Mag.*, **26**, 73–89.

Kawamura, R., 1984: Relation between atmospheric circulation and dominant sea surface temperature anomaly patterns in the North Pacific during the Northern Hemisphere winter. *J. Meteor. Soc. Japan*, **62**, 910–916.

———, 1986: Seasonal dependency of atmosphere-ocean interaction over the North Pacific. *J. Meteor. Soc. Japan*, **64**, 363–371.

Lanzante, J.R., 1984: A rotated eigenanalysis of the correlation between 700 mb heights and sea surface temperatures in the Pacific and Atlantic. *Mon. Wea. Rev.*, **112**, 2270–2280.

Love, G., 1985: A study of the linear relationships between the monthly mean fields of sea surface temperature, mean sea level pressure and cloudiness over the Northwest Pacific. *J. Meteor. Soc. Japan*, **63**, 201–209.

Michaelsen, J., 1982: A statistical study of large-scale, long-period variability in North Pacific sea surface temperature anomalies. *J. Phys. Oceanogr.*, **12**, 694–703.

Namias, J., 1959: Recent seasonal interactions between North Pacific waters and the overlying atmospheric circulation. *J. Geophys. Res.*, **64**, 631–646.

———, 1969: Seasonal interactions between the North Pacific Ocean and the atmosphere during the 1960's. *Mon. Wea. Rev.*, **97**, 173–192.

———, 1970: Macroscale variations in sea-surface temperatures in the North Pacific. *J. Geophys. Res.*, **75** 565–582.

———, 1971: The 1968–69 winter as an outgrowth of sea and air coupling during antecedent seasons. *J. Phys. Oceanogr.*, **1**, 65–81.

———, 1973: Thermal communication between the sea surface and lower troposphere. *J. Phys. Oceanogr.*, **3**, 373–378.

———, 1975: Stabilization of atmospheric circulation pattern by sea surface temperatures. *J. Mar. Res., supplement*, 53–60.

———, 1978: Multiple causes of the North American abnormal winter 1976–77. *Mon. Wea. Rev.*, **106**, 279–295.

———, 1980: Causes of some extreme Northern Hemisphere climatic anomalies from summer 1978 through the subsequent winter. *Mon. Wea. Rev.*, **108**, 1333–1346.

———, and B. Born, 1970: Temporal coherence in North Pacific sea surface temperature pattern. *J. Geophys. Res.*, **75**, 5952–5955.

Nishihashi, H., and I. Imai, 1985: Variations of sea surface temperatures in the North and Equatorial Pacific (in Japanese with English abstract and figure captions). *J. Faculty of Marine Science and Technology, Tokai Univ.*, **21**, 1–16.

North, G.R., T.L. Bell, R.F. Cahalan, and F.J. Moeng, 1982: Sampling errors in the estimation of empirical orthogonal functions. *Mon. Wea. Rev.*, **110**, 699–706.

Pitcher, E.J., M.L. Blackmon, G.T. Bates, and S. Munos, 1986: The effects of midlatitude Pacific sea-surface temperature anomalies on the January climate of a general circulation model. *J. Atmo. Sci.*, (in press.)

Preisendorfer, R.W., F.W. Zwiers, and T.P. Barnett, 1981: *Foundations of principal component selection rules, SIO Ref. Ser. 81–4*, Scripps Institution of Oceanography.

Prohaska, J.T., 1976: A technique for analysing the linear relationships between two meteorological fields. *Mon. Wea. Rev.*, **104**, 1345–1353.

Reynolds, R.W., 1978: Sea surface temperature anomalies in the North Pacific Ocean. *Tellus*, **30**, 97–103.

Roden, G.I., and G.W. Groves, 1960: On the statistical prediction of ocean temperatures. *J. Geophys. Res.*, **65**, 249–263.

Saiki, M., and K. Nagasaka, 1986: Long-term variations of sea surface temperature in the North Pacific Ocean. *Oceanogr. Mag.*, **36**, 51–55.

Saur, J.F.T., 1980: Surface salinity and temperature on the San Francisco – Honolulu route June 1966 – December 1970 and January 1972 – December 1975. *J. Phys. Oceanogr.*, **10**, 1669–1680.

Storch, H., and G. Hannoschöck, 1985: Statistical aspects of estimated principal vectors (EOFs) based on small sample sizes. *J. Climate Appl. Meteor.*, **24**, 716–724.

Wallace, J.M., and D.S. Gutzler, 1981: Teleconnections in the geopotential height field during the Northern Hemisphere winter. *Mon. Wea. Rev.*, **109**, 784–812.

Weare, B.C., 1977: Empirical orthogonal analysis of Atlantic Ocean Ocean surface temperatures. *Qurt. J.R. Met. Soc.*, **103**, 467–478.

———, A.R. Navato, and R.E. Newell, 1976: Empirical orthogonal function analysis of the Pacific Ocean surface temperatures. *J. Phys. Oceanogr.*, **6**, 671–678.

White, W.B., and R.L. Bernstein, 1979: Design of and oceanographic network in the midlatitude North Pacific. *J. Phys. Oceanogr.*, **9**, 592–606.

———, and A.E. Walker, 1974: Time and depth

scales of anomalous subsurface temperature at ocean weather stations, P, N, and V in the North Pacific. *J. Geophys. Res.*, **79**, 4517–4522.

————, R. Bernstein, G. McNally, S. Pazan, and R. Dickson, 1980: The thermocline response to transient atmospheric forcing in the interior midlatitude North Pacific 1976–1978. *J. Phys. Oceanogr.*, **10**, 372–384.

————, G. Meyers, and K. Hasunuma, 1982: Space/time statistics of short-term climatic variability in the western North Pacific. *J. Geophys. Res.*, **87**, 1979–1989.

————, G.A. Meyers, J.R. Donguy, and S.E. Pazan, 1985: Short-term climatic variability in the thermal structure of the Pacific Ocean during 1979–1982. *J. Phys. Oceanogr.*, **15**, 917–935.

1969年～1979年の北太平洋表面水温アノマリの解析およびその変動と北半球500 mb 高度場アノマリとの関係

岩坂直人・花輪公雄・鳥羽良明

（東北大学理学部地球物理学教室）

北太平洋月平均5°×5°格子データセットを日本海洋データセンター提供の表面水温資料から新たに計算し，北太平洋の表面水温アノマリの変動の特徴および北半球500 mb 高度場の変動との関係について調べた。表面水温アノマリパターンの代表的な空間スケールは東西約数千km，南北1～2千kmである。典型的な表面水温アノマリパターンはその出現から数ヵ月ないし一年ほど追跡できる。スペクトル解析の結果は，表面水温アノマリには数年程度の周期の変動も存在することを示した。表面水温アノマリは広範囲にわたりほぼ同時に出現し移動拡大するが，その速さや方向には明白な規則性は存在しないように見える。ただし，時期を限って見れば，表面水温アノマリパターンが移流によって動いていると考えることのできる場合もある。

表面水温アノマリの主成分解析によると，第1主成分は北太平洋の中央付近を中心とする同心楕円状の空間パターンを持つ。係数の時系列は数ヵ月と数年の周期の変動が卓越するが，1972／73 El Niño event に相当するピークはみられない。本研究の主成分解析結果は Davis (1976)の研究結果と一致するが，研究対象海域に赤道域を含む Weare et al. (1976) や Kawamura (1984) の結果とは多少異なっている。

表面水温の変動は北半球500 mb 高度場の変動と高い相関があり，ラグ相関解析の結果によると北太平洋の表面水温アノマリの第1主成分の変動は大気のＰＮＡテレコネクションパターンを示す変動に起因すると考えられる。